UNIVERSITÉ DE GENÈVE

Archive ouverte UNIGE
https://archive-ouverte.unige.ch

Article scientifique | Article | 2019

Published version | Open Access

This is the published version of the publication, made available in accordance with the publisher's policy.

Quantification of Colorimetric Data for Paper-Based Analytical Devices

Soda, Yoshiki; Bakker, Eric

How to cite

SODA, Yoshiki, BAKKER, Eric. Quantification of Colorimetric Data for Paper-Based Analytical Devices. In: ACS Sensors, 2019, vol. 4, n° 12, p. 3093–3101. doi: 10.1021/acssensors.9b01802

This publication URL: https://archive-ouverte.unige.ch/unige:142024
Publication DOI: 10.1021/acssensors.9b01802

© This document is protected by copyright. Please refer to copyright holder(s) for terms of use.

ACS SENSORS

Perspective

Cite This: ACS Sens. 2019, 4, 3093−3101

pubs.acs.org/acssensors

Quantification of Colorimetric Data for Paper-Based Analytical Devices

Yoshiki Soda and Eric Bakker*

Department of Inorganic and Analytical Chemistry, University of Geneva, Quai Ernest-Ansermet 30, CH-1211 Geneva, Switzerland

Supporting Information

ABSTRACT: Colorimetric measurements by image analysis, giving RGB or HSV data, have become commonplace with optical indicator-based assays and as a readout for paper-based analytical devices (PADs). Yet, most works on PADs tend to ignore the quantitative relationship between color data and concentration, which may hamper their establishment as analytical devices and make it difficult to properly understand chemical or biological reactions on the paper substrate. This Perspective Article discusses how image color data are computed into colorimetric absorbance values that correlate linearly to dye concentration and compare well to traditional spectrophotometry. Thioflavin T (ThT), Neutral Red (NR), and Orange IV are used here as model systems. Absorbance measurements in solution correlate well to image data (and Beer's law) from the color channel of relevance if the gamma correction normally used to render the picture more natural to the human eye is removed. This approach also allows one to correct for color cast and variable background color, which may otherwise limit quantitation in field measurements. Reflectance measurements on paper color spots are equally found to correlate quantitatively between spectroscopy and imaging devices. In this way, deviations from Beer's law are identified that are explained with dye interactions on the paper substrate.

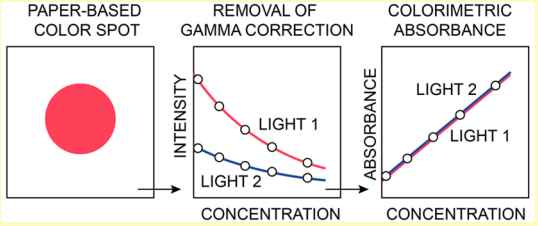

KEYWORDS: *colorimetry, RGB analysis, scanner, gamma correction, background light correction, smartphone analysis, paper-based analytical devices*

Downloaded via UNIV OF GENEVA on September 17, 2020 at 07:29:04 (UTC).
See https://pubs.acs.org/sharingguidelines for options on how to legitimately share published articles.

Microfluidic paper-based analytical devices (μPADs), introduced in 2007 by Whitesides, are simplified variants of lab-on-a-chip (LOC) devices.[1] Because they tend to employ chromogenic reagents as indicators in most reported cases, colorimetry has been the most-used technique for analyte quantification on paper. For this reason, signal acquisition typically relies on external equipment such as a camera, scanner, or smartphone.[2,3] Because the final colorimetric signal varies with the specific device and light source, experimental data is difficult to cross-correlate. To help overcome this limitation, equipment-free semiquantification has been explored that may output distance-,[4−7] text-,[8−10] timing-,[11−13] and counting-based[14−16] signals with the help of chromogenic reagents. Despite these advances, many PAD principles are difficult to convert to these types of readouts and still require traditional colorimetric detection.

Unfortunately, most work on paper-based sensors has not strongly focused on the acquired color of the image data for quantitation, even though the response on paper substrate tends to deviate from ideal behavior.[17−22] Also, quantitative image analysis is known to be difficult in inconsistent lighting conditions, which is an important limitation for the practical acceptance of PADs.[23] It is therefore important to acquire a colorimetric signal that can be correlated to spectrophotometric absorbance values. This would allow one to use image data by means of a camera detector to evaluate Beer's law in solution and on a substrate of choice. It would also help researchers on PADs understand the influence of the paper substrate on the chemistry of indicator readout.

This Perspective Article aims to help clarify how image data are best reported for quantitative analysis by first discussing the simpler case of homogeneous solution phase and subsequently moving to paper-based substrates. The concept of gamma correction and the need for its removal are discussed. Pixel intensities are converted to a more robust absorbance value that is less dependent on color background. The resulting data are successfully correlated to spectrophotometry, both for solution phase and reflectance with paper substrates.

This Perspective Article builds on earlier work. The computing of absorbance values from image data has been reported earlier,[24,25] as is the need for the removal of gamma correction for accurate color analysis.[26−30] The removal of gamma correction has been reported to be important for understanding the behavior of a chemical reaction[26,27,30] because the color produced on the image without gamma correction reflects the actual light intensity. Unfortunately, these same reports lacked a direct comparison of the color calculated from the spectrum of the dye with the experimental color from the image data;[27,28,30] therefore, the validity of gamma removal was not assessed. Some works compared the absorbance spectra

Received: September 16, 2019
Accepted: November 20, 2019
Published: November 20, 2019

© 2019 American Chemical Society

DOI: 10.1021/acssensors.9b01802
ACS Sens. 2019, 4, 3093−3101

of the dye and resulting absorbance calculated by RGB values,[26,31] but they are not strictly comparable parameters because the calculation methods to obtain absorbance from spectrophotometry or RGB-based image data are different, as will be discussed here. Out of the works mentioned above, Christodouleas et al. demonstrated the correlation of RGB-analyzed and spectrophotometer-based absorbance in well-defined aqueous solutions, taking into account gamma correction and RGB sensitivity.[32] We summarize here these findings and further demonstrate how absorbance values from RGB data can be made to correlate to spectrophotometry. Colorimetric absorbance is shown to be independent of variable background color. An experimental approach to record the spectral sensitivity and gamma correction of smartphone cameras is proposed. Furthermore, image data from paper-based substrates are correlated successfully to reflectometry, which helps quantify to what extent dye-colored paper spots may deviate from Beer's law.

RESULTS AND DISCUSSION

Elimination of Gamma Correction. When image data are taken by a camera, the output color on the screen does not directly reflect the detected light intensity from the object. The data are curved by gamma (γ) correction to make the resulting picture on the screen look natural to the human eye. This exponential correction is according to Weber–Fechner's law.[33] Therefore, the output light intensity is not proportional to the input intensity as shown in Figure 1.

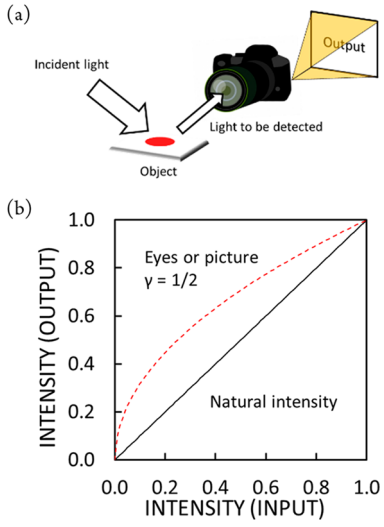

Figure 1. (a) Illustration of a colorimetric detection system where a picture is taken and output on a screen and (b) relationship between input and output light intensity in the absence (black line) and presence (dashed line) of gamma correction.

Consequently, once a camera detects reflected light from the subject, it is subjected to gamma correction (Figure 1b), described by eq 1

$$I_{output} = I_{input}^{\gamma} \tag{1}$$

where I_{output} and I_{input} are the relative light intensities of the output and input, respectively, normalized to range from 0 to 1. The corresponding absorbance may be obtained by taking into account I_0 as the light output for when the object does not contain the absorbing substance. For the color channel of interest, the absorbance is written as

$$A = -\gamma \log(I_{output}/I_0) \tag{2}$$

The coefficient γ corresponds to the gamma correction of both intensities shown. When a camera outputs a color, it aims to approach the sensitivity of our eyes to red, green, and blue color. The detected light intensity I_{input} is converted by this sensitivity to the biased intensity I_{input}'. Figure S1 shows the theoretical spectral sensitivity of RGB color space (sRGB obtained with the standard illuminant C) at each wavelength obtained by an algebraic conversion from XYZ tristimulus values proposed by CIE (Commission internationale de l'éclairage) in 1931 with primaries at 645.16, 526.32, and 444.44 nm. In this paper, this color function defined by sRGB (illuminant C) was employed because the spectrum conversion by this color function derived well-correlating absorbance values in all RGB channels with those from the imaging device.

The absorbance value calculated from either I_{input} and I_{input}' should be the same because the sensitivity bias equally multiplies I_{input} and I_0; see eq 2. In an 8-bit jpeg file, the intensities I_{input}' integrated over the window of wavelengths are expressed as R, G, or B with a value ranging from 0 to 255. RGB values, therefore, have the same fundamental meaning as light intensity. Gamma-corrected RGB values may therefore be used to calculate absorbance values as follows:

$$\mathrm{R,G,B}_{output} = 255\left(\frac{\mathrm{R,G,B}_{input}}{255}\right)^{\gamma} \tag{3}$$

$$A_{\mathrm{Red,Green,Blue}} = -\gamma \log(\mathrm{R,G,B}_{output}/\mathrm{R}_0, \mathrm{G}_0, \mathrm{B}_0) \tag{4}$$

The division by 255 in eq 3 is needed because gamma correction is applied to an intensity range of 0 to 1, as mentioned above.

Absorbance values calculated from RGB image analysis on the basis of eq 4 can be correlated to spectrophotometric absorbance. We note, however, that molar absorptivity is wavelength-dependent and in the general case the wavelength maximum does not perfectly overlap with a given color channel of the imaging detector. The correlation shown in Figure 2 is using the dye ThT at different concentrations, chosen because it gives a simple spectrum in the blue channel. To calculate the absorbance value, the blue channel light intensities (solid lines in Figure 2a) were computed from the spectrophotometric intensity data (broken lines in Figure 2a) by multiplying each recorded intensity spectrum with the spectral sensitivity of the blue channel (Figure S1b). In this manner, the values of spectrophotometric intensity obtained from the spectrophotometer was converted as follows:

$$I_{blue}(\lambda) = I_{origin}(\lambda)\, B(\lambda) \tag{5}$$

where $I_{blue}(\lambda)$ and $I_{origin}(\lambda)$ are blue-channel corrected and the original light intensity and $B(\lambda)$ is the spectral sensitivity of the relevant RGB color function (see Figure S1b) of the imaging device. The converted light intensity (solid line in Figure 2a) was integrated over all the wavelengths as shown in Figure S3a, correlating well to the blue values obtained from image data (Figure S3b) when $\gamma = 1$. The discrepancy of the values originates in the different definition of the output value and is overcome by use of eq 4 to obtain colorimetric absorbance data. Those are found to correlate well with colorimetric absorbance from the blue channel of the imaging device (black circles in Figure 2b) if gamma correction is removed ($\gamma = 1$).

DOI: 10.1021/acssensors.9b01802
ACS Sens. 2019, 4, 3093−3101

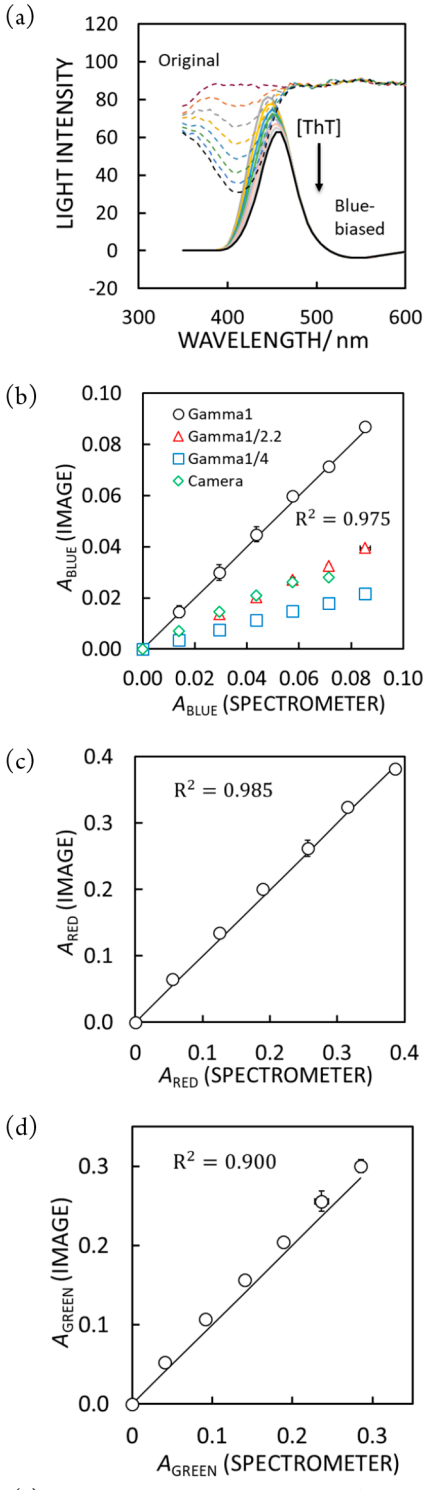

Figure 2. (a) Intensity spectrum observed by the spectrophotometer (dashed line) is shown together with the simulated biased intensity in the blue channel of the RGB color space (solid line). (b) Comparison of the blue-channel corrected absorbance values from spectrophotometry (x-axis) to blue channel colorimetric absorbance acquired with a CanoScan 9000f Mark II scanner with gamma correction of 1 (black circles), 1/2.2 (red triangles), and 1/4 (blue squares) and with the Cannon EOS 40D camera (green diamonds). Figure S2a–d shows actual analyzed image data. Comparison of the (c) red-channel and (d) green-channel corrected absorbance values from spectrophotometry (x-axis) of Methylene Blue (MB) and Neutral Red (NR), respectively, to those values acquired by CanoScan 9000f Mark II scanner without gamma correction. Error bars are standard deviations ($n = 3$). The slope of theoretical line (black line) in each figure is 1. The slope of the fitted line and the corresponding R^2 value are, respectively, (b) 1.018 and 1.000, (c) 1.019 and 0.997, and (d) 1.078 and 0.997.

Note that the blue channel corresponds to a shoulder of the original intensity spectrum, giving larger uncertainties than absorbance values calculated from peak maxima. Consequently, blue channel absorbance is equivalent to an absorbance measurement at a specific wavelength, different from peak maximum. This absorbance has been referred to as "RGB-resolved absorbance"[32] or "relative absorbance analogues"[24] in the literature and is here simply called colorimetric absorbance. The dye ThT gives much smaller recorded light intensity changes in the red and green channels (Figure S4). Figure 2b shows that only data without gamma correction ($\gamma = 1$) give satisfactory correlation with spectrophotometry. A higher gamma correction (lower values of γ) lowers the observed absorbance of the imaging device in agreement with eq 4. Note the deviation with data from an imaging camera (Cannon EOS 40D camera) caused by a proprietary gamma correction function that does not strictly follow the form given in eq 4. The function of algebraic conversion from XYZ tristimulus color function to each RGB color function is usually reported. One must be aware that, similar to gamma correction, color-matched RGB values equally impose a correction on the detected light which may cause a deviation from Beer's law from the original RGB color function (Figure S5).

Analogous investigations for the red channel with Methylene Blue (MB) and for the green channel with Neutral Red (NR) also showed good correlations (see Figure 2c and d) similar to the blue channel with ThT, which supports here the use of the sRGB (illuminant C) color function. The original spectrum of the dye should adequately overlap with the spectral RGB sensitivity to obtain good correlations as shown in Figure S6. It is important to choose a channel to which the dye of interest is sufficiently responsive.

Gamma Correction and Spectral Sensitivity of Smartphones. The spectral sensitivity and the gamma correction algorithm of modern smartphones tend to be proprietary and are not disclosed by the manufacturer. It is here proposed to characterize the spectral sensitivity spectrum of a smartphone by recording a timed movie in a spectrophotometer while sweeping the wavelength of the light in a predefined range and scan rate. Each recorded movie frame may be assigned to the appropriate wavelength as follows:

$$\lambda(n_f) = \lambda_0 + n_f \mathrm{fps}^{-1} v_{\mathrm{scan}} \quad (6)$$

where λ is the wavelength of the light, λ_0 is the starting wavelength of the scan in nm, n_f is the video frame number, fps is the number of video frames recorded per second, and v_{scan} is the scan rate in nm s^{-1}. Software analysis of the movie frames allows one to extract the sensitivity spectrum for each RGB color channel, as shown in Figure 3a for the iPhone XR smartphone as example.

Figure 3b–d shows the correlation of RGB absorbance values calculated from spectrophotometric and smartphone image data from an iPhone XR smartphone. As gamma correction is typically not known with smartphones, they may be determined by this absorbance correlation. Because the applied gamma correction value may vary depending on ambient light and other

DOI: 10.1021/acssensors.9b01802
ACS Sens. 2019, 4, 3093–3101

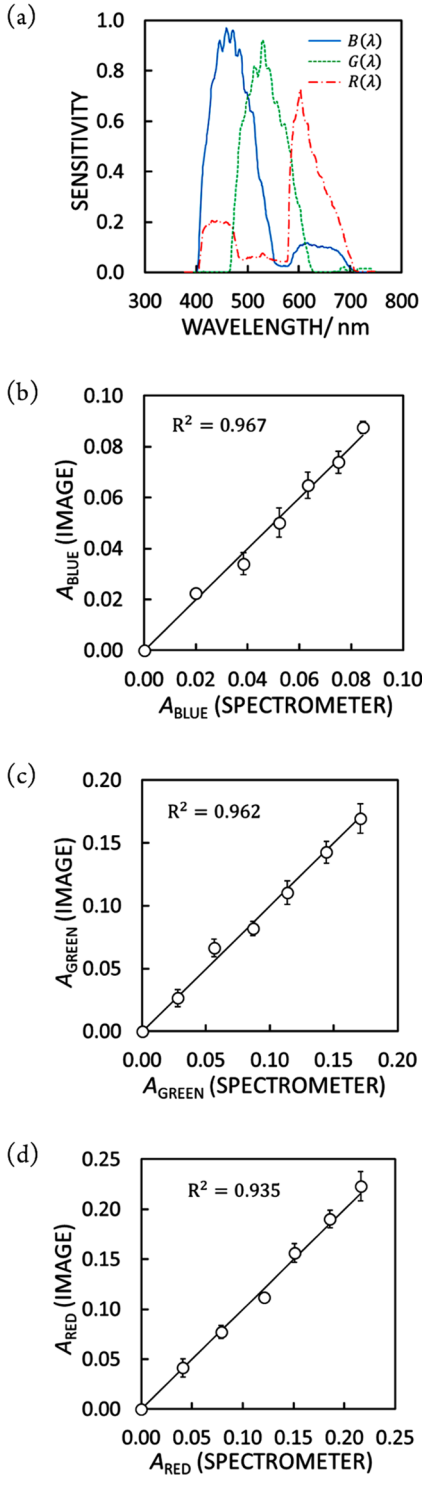

Figure 3. (a) RGB color function of iPhone XR smartphone where the blue solid represents blue sensitivity $B(\lambda)$, green dashed line represents $G(\lambda)$, and red long-dashed/dot line represents $R(\lambda)$. (b–d) Comparison of RGB absorbance values from spectra (x-axis) and image (y-axis) data in blue, green, and red channels, respectively. Error bars are standard deviations (n = 3). The standard deviation in the x-axis direction is given in each plot. See Figure S2g for the actual image of the ThT solution used in this experiment. Determined gamma correction values were used with eq 4 for the calculation in (b)–(d). Slopes of theoretical straight lines shown are unity. The slopes and corresponding R^2 values for the least-squares fits (intercept of zero) are, respectively, (b) 1.002 and 0.993, (c) 0.991 and 0.994, and (d) 1.015 and 0.996.

automated settings, it is recommended to maintain consistent experimental lighting conditions when investigating this characteristic.

For Figure 3, the mean value of the gamma correction obtained by eq 2 was used to represent the gamma correction of each color channel. For the iPhone smartphone, they were determined as γ_{Blue} = 1/2.38, γ_{Green} = 1/2.27, and γ_{Red} = 1/1.58 for the blue, green, and red channels, respectively. Gamma correction values are generally in the range of 2.0–2.2, but discrepancies from the typical value and inconsistencies among channels have been reported earlier.[32] The relatively high correction value for the red channel (γ_{Red}) means that the camera stresses purposely its color over those in the other two channels.

The approaches given here make it possible to obtain the spectral sensitivity as well as the gamma correction values for consumer level detection devices such as smartphones that are becoming important in low cost analytics such as paper-based assays and sensors.

Independence of RGB Absorbance on Background Color. Absorbance data (eq 2) should be much less dependent on the intensity or color of the broad background light than simple RGB values, since light variations are reasonably corrected by forming the intensity ratio, I/I_0.

The absorbance changes as a function of concentration with widely different color backgrounds are shown in Figure 4c. Even with obviously different background colors (Figure 4a) that give highly inconsistent blue values (see Figure 4b), absorbance values remain very similar to the values taken with a white background (all data without gamma correction at γ = 1), and are within 5.1% to each other (average values in Figure 4c). This approach may help overcome the reported problem of variable background light in colorimetric analysis and is highly recommended for quantitative work.[23]

Quantifying RGB Images on Paper. Paper-based analytical devices show color spots that are observed by reflected, rather than transmitted light. Reflectance spectrophotometry can be used to correlate to RGB image data in the same general manner as for the transmission experiments shown above. For this purpose, paper spots were colored with ThT dye at different loadings. In analogy to the procedure used for Figure 2, the recorded spectrum was filtered by the blue channel sensitivity (see Figure S7 for details) to arrive at the spectrophotometrically predicted intensity change of the blue channel. The recorded reflectance spectra for different ThT concentrations on paper (Figure 5a) give blue channel absorbance values (x-axis on Figure 5b) that correspond well to that observed by the imaging device (see y-axis on Figure 5b). The blue channel light intensities or blue values vs dye concentration for the two methods are shown in (Figures S7c and S8), where the integrated blue-biased light intensities (see Figure S7c) and blue values from the imaging device (see Figure S8) give analogous behavior to the solution phase discussed above.

In addition, Neutral Red (NR), a dye responsive in both red and green channels on paper substrate was investigated in analogy; see Figure S9 for the associated spectra. Figure 5c and d shows very good correlation of the red and green values obtained from reflectance measurement and image data. Therefore, as with the transmission experiments described above, quantification of colorimetric data is possible by correlation with spectrophotometry given adequate spectral overlap.

DOI: 10.1021/acssensors.9b01802
ACS Sens. 2019, 4, 3093–3101

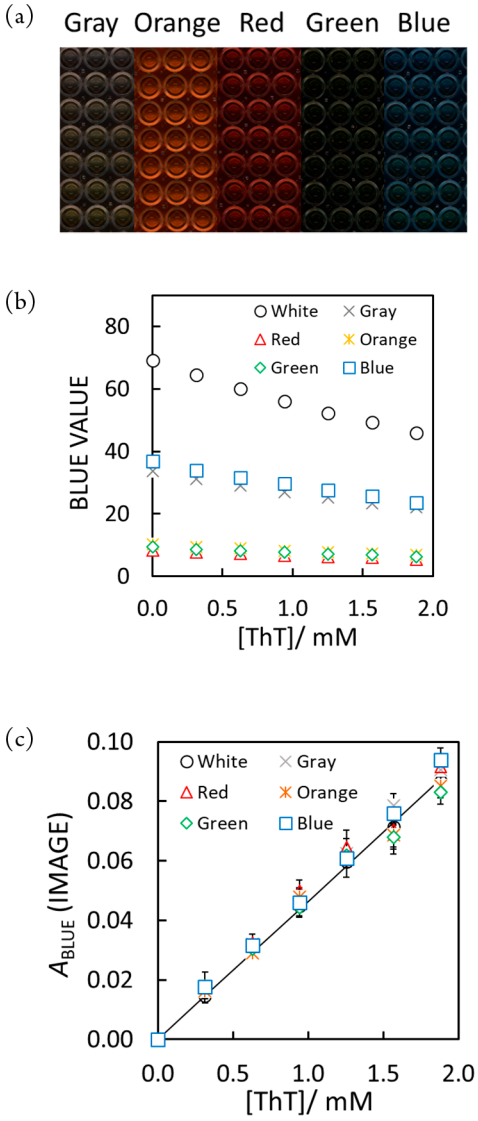

Figure 4. (a) Recorded images of a 96 well plate holding ThT solutions of 0, 100, 200, 300, 400, 500, and 600 mg/L from the bottom to the top with indicated color backgrounds, acquired with a gamma correction value of 1; in other words, without gamma correction according to eq 1. (b) Analyzed blue intensity values for each color background of (a), showing large deviations caused by the variable color background. (c) Corresponding colorimetric absorbance values for the same ThT solution with variable color background, resulting in a dramatic decrease of variability. Error bars are standard deviations (n = 3).

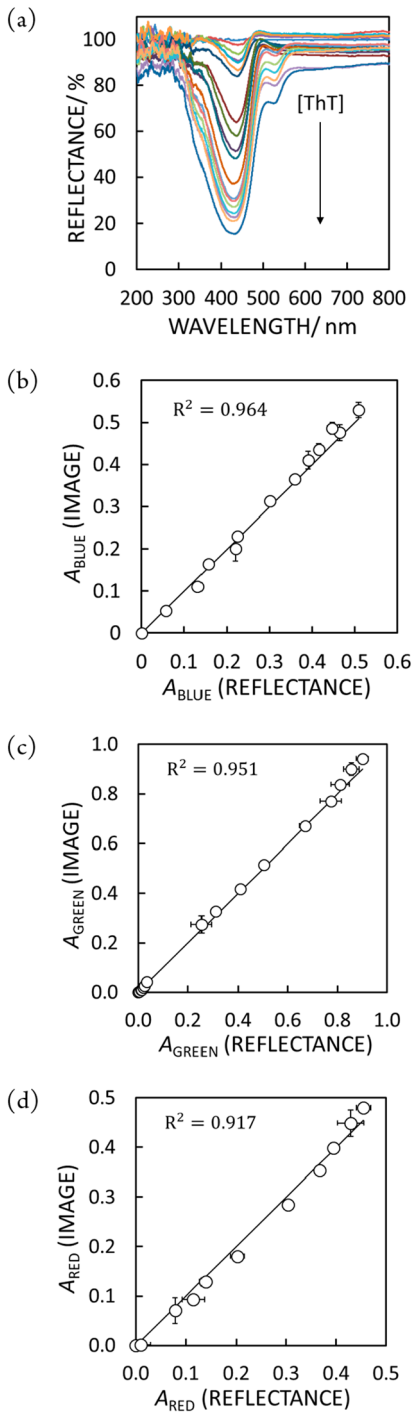

Figure 5. (a) Reflectance spectra of ThT-colored paper spots, (b) comparison between the resulting blue-channel corrected absorbance and colorimetric absorbance in analogy to Figure 2, and (c) same comparison of red and green channel with Neutral Red (NR)-colored paper spots. Figure S2e and f shows the actual analyzed image data. Error bars are standard deviations (n = 3). The slope of theoretical line (black line) in each figure is unity. The slopes and the corresponding R^2 value for the least-squares fit (intercept of zero) are, respectively, (b) 1.038 and 0.995, (c) 1.031 and 0.999, and (d) 1.002 and 0.994.

Neutral Red is not sufficiently responsive for the red channel in aqueous solution but does show a signal on the paper substrate that is caused by a spectral shift from solution phase (Figure S4b) to the paper substrate (Figure S9) as discussed below.

Behavior of Dye-Adsorbed Paper. Fundamentally, colorimetric reflectance data correlate well to spectrophotometry. Nonetheless, absorbance is not found to increase linearly with the ThT concentration on paper as expected from Beer's law, see Figure 6a. Instead, linear behavior is confirmed only at higher dilution in Figure 6b. This suggests that the observed nonlinearity is caused by chemical interactions. The ratio of suppressed to ideal absorbance, or deterioration ratio, is calculated based on reflectance and RGB analysis (Figure S10b) and shows the same result. The color of the dye on paper behaves differently from that in the solution phase.

Neutral Red (NR) and Orange IV are both substantially responsive in the blue channel and were investigated to further

DOI: 10.1021/acssensors.9b01802
ACS Sens. 2019, 4, 3093−3101

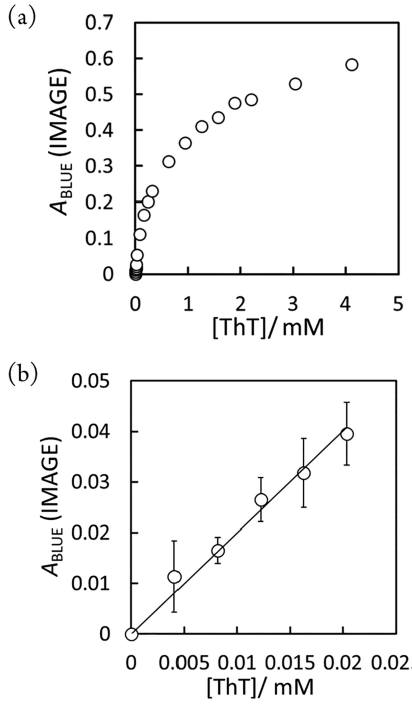

Figure 6. (a) Blue-channel corrected absorbance value of Thioflavin T (ThT) from the image data taken with the CanoScan 9000f Mark II scanner and (b) linearity of colorimetric absorbance calculated from RGB image analysis of ThT-colored spots at low concentration. Error bars are standard deviations (n = 3). The slope and R^2 value of (b) are 2.001 and 0.984, respectively.

substantiate this phenomenon (Figure 7b, c). Orange IV exhibits a very similar absorbance peak to ThT (see Figure S11). The responsivity of NR in the blue channel is only slightly inferior to that in the green channel.

Neutral Red (electrically neutral) and Orange IV (negatively charged, pK_a: 2.0[35]) were chosen to evaluate their chemical interaction with cellulose (negatively charged; pK_a 3.0−5.0[36,37]) and solubility. The deviation may be caused by aggregation of the dye on the paper substrate. As this interaction can be electrical or hydrophilic, dyes with different valencies, +1, 0, −1 were chosen. In the absence of charge differentiation, the hydrophilicity of the dyes may also drive aggregation. In agreement with the solubility order (Figure 7b),[34] Orange IV is more hydrophobic than the other two dyes as it was no longer soluble at 2.2 mM, in contrast to ThT, which in turn is less soluble than Neutral Red.

Figure 7c indicates that the deviation from Beer's law at increasing concentrations may be generally observed for most dyes, the extent of which depends on dye structure. We suspect that the deviation is most probably caused by π-stacking of the dye due to the aggregation on the paper. Looking carefully into the reflectance spectrum of ThT (see Figure 5a), there is a generation of the new peak around 540 nm which is found outside of the blue channel sensitivity. This can be considered a gradual absorbance peak shift from the initial 410−550 nm as ThT is concentrated on the paper substrate. Absorbance peaks have indeed been found to shift dramatically in the presence of π-stacking of the dye with other substances.[38] Interactions between ThT and the substance without causing π-stacking may prevent this absorbance shift, as in water, where each ThT molecule interacts only with water molecules. The same

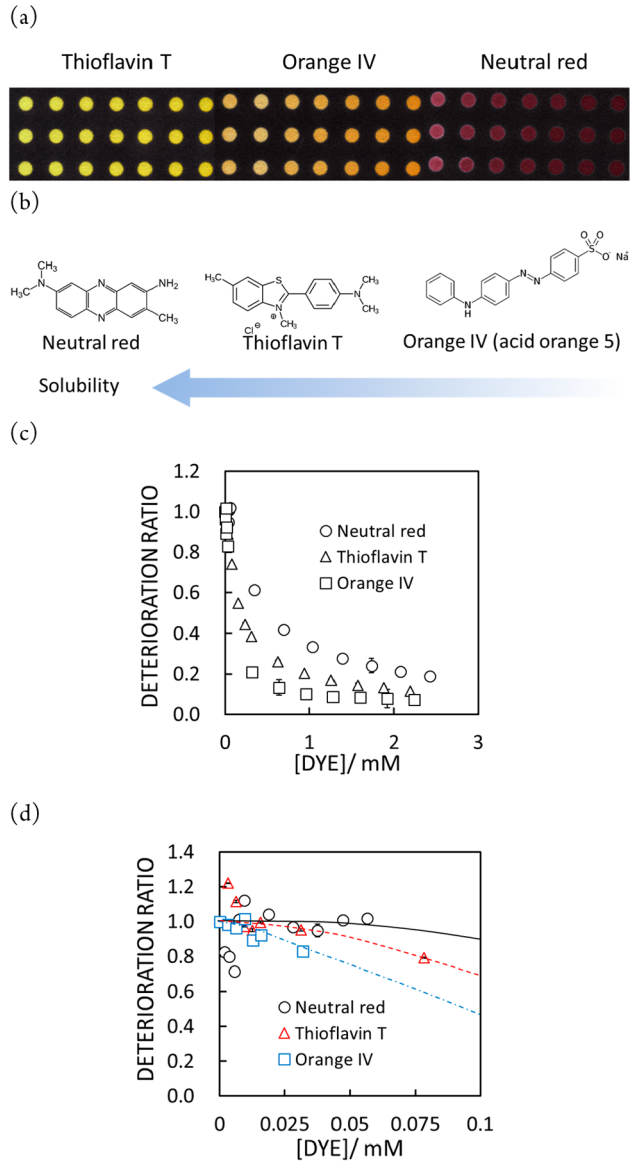

Figure 7. (a) Recorded image of paper spots colored by 8 μL of ThT, Orange IV, and Neutral Red aqueous solutions of 100, 200, 300, 400, 500, 600, and 700 mg/L, from left to right respectively; (b) structures of the dyes used for the investigation of deterioration ratio in the order of increasing solubility; (c) deterioration ratio obtained with each dye and (d) deterioration ratio as a function of concentration for each dye at low concentration, where the black line, red dashed line, and blue long-dashed/dot line indicate the behavior of Neutral Red, Thioflavin T, and Orange IV, respectively. Solubility was estimated by ADME provided by the Swiss Institute of Bioinformatics.[34] Error bars are standard deviations (n = 3).

phenomenon was seen with Neutral Red on paper substrate as mentioned above, where the spectrum on the paper is broader than that for aqueous solution phase; see Figures S4b and S9.

The discussion assumes that dyes homogeneously distribute through the thickness after the spots were dried. Positively charged Thioflavin T may interact with negatively charged carboxylic groups and cause a chromatographic effect in the thickness direction of the paper. Such an effect was not observed in the cross section image of the ThT-colored paper spot; see Figure S12 as dyes uniformly distribute through the paper.

DOI: 10.1021/acssensors.9b01802
ACS Sens. 2019, 4, 3093−3101

Accordingly, we advocate that the more hydrophilic dye can better interact with the hydrophilic cellulose fiber and π-stacking under dried condition can be alleviated to some extent. This hypothesis agrees with the result shown in Figure 7c, where most hydrophilic dye Neutral Red has less absorbance deterioration followed by ThT and Orange IV in the order of hydrophilicity.

As shown in Figure 7d, Beer's law may be fulfilled under dilute conditions, with Neutral Red exhibiting linearity in a wider range of concentrations, followed by ThT and Orange IV, in the order of decreasing hydrophilicity.

Dye aggregation can be partly reversed by the addition of water, as demonstrated with ThT in Figure 8. In practice, this suggests that the wetness of the paper may need to be controlled for consistent colorimetric analysis.

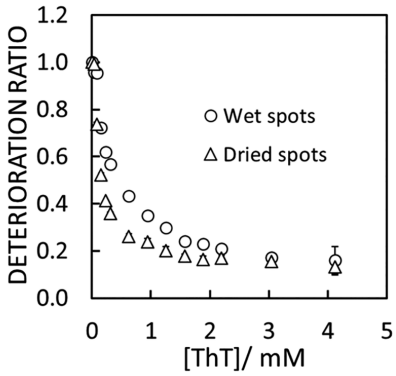

Figure 8. Deterioration ratio obtained with ThT on the paper spots under dried and wet conditions by applying 2 μL of water. Error bars are standard deviations (n = 3).

CONCLUSIONS

Colorimetric detection via a digital camera, smartphone, or flatbed scanner has become a cornerstone for the realization of low-cost analytical devices. This Perspective Article aims to give some recommendations to make this type of readout as robust as possible, using transmission with microtiter plates and reflectance with paper-based devices as concrete examples. A correlation between established spectrophotometry and colorimetric detection may be found successfully by taking into account the spectral sensitivity of a given color channel of the imaging device. This makes it possible to evaluate the validity of Beer's law and find optimal protocols for practical use.

To allow for best quantification of colorimetric data, the imaging device must allow for removal of gamma correction, which is a function applied to render images more natural to the human eye. Unfortunately, photographic cameras may apply proprietary curves to the acquired image data that make them poor choices for quantitative analysis. Color matching functions similarly manipulate the data and should be avoided.

As shown here, it is possible to acquire the spectral sensitivity of the colorimetric detector by recording a movie in a spectrophotometer, as shown here with an iPhone XR smartphone. This information allows one to also arrive at the gamma correction information by correlating to spectrophotometric absorbance data. For Canon EOS cameras, third party software such as Magic Lantern may help with controlling camera settings including gamma correction.

For best quantitative results, one should choose a color channel as closely aligned to the absorbance maximum of the dye. Any spectral deviation will invariably result in a decrease of sensitivity relative to established, uncorrected spectrophotometry.

Importantly, it is recommended to report colorimetric data as absorbance values by calculating the logarithm of the intensity of the color spot divided by the intensity of a spot of the same substrate illuminated by the same light but without colorimetric reagent. This gives colorimetric absorbance values that should be proportional to dye concentration, in analogy to spectrophotometry. This approach allows one to effectively correct for variable background lighting conditions and is recommended for quantitative work.

The reporting of colorimetric absorbance values on paper substrates follows the same general guidelines as for transmission experiments. This allows one to evaluate whether linearity with dye concentration is fulfilled, and if not, to assess the fundamental reasons for any deviation. In this specific study, dye aggregation by π-stacking is thought to result in a deviation from linearity at higher loadings on paper.

If the function between dye concentration and absorbance is properly identified on a given substrate, one should be able to identify the amount of dye in a given chemical form just by analyzing the entire color image, without the need for any particular paper channels or spot shapes, which would greatly simplify quantitative analysis. This work is currently in progress in our laboratory.

EXPERIMENTAL SECTION

Materials and Instruments. Thioflavin T (ThT), Neutral Red (NR), and Orange IV were purchased from Sigma-Aldrich (St. Louis, MO). Methylene Blue was purchased from Alfa Aesar (Haverhill, MA). Ultrapure water (>18 MΩ cm) was obtained from a PURELAB flex water purification system (ELGA, Veolia Water, Marlow, U.K.). A 96-well plate (Grenier Cellstar) was sourced from Greiner bio-one (Kremsmunster, Austria). Absorbance measurement was performed by using a Spectra Max M5 instruments (Molecular Devices, Danaher, San Jose, CA) and the corresponding software SoftMax Pro. A Canon EOS 40D camera equipped with an EF 35 mm f/2 IS USM lens, a Canon (Tokyo, Japan) EOS 5D Mark III camera equipped with an EF 200 mm f/4 IS USM lens followed by a microscope lens Plan-neofluor 10×/0.30, and a CanoScan 9000f Mark II scanner were purchased from Canon. Whatman No. 4 qualitative grade filter paper was purchased from GE Healthcare UK Limited (Buckinghamshire, U.K.). CorelDraw software was used to pattern paper spots on the paper substrate (Whatman No. 4). Hydrophobic wax was printed on Whatman No. 4 paper by using a Xerox Colorqube 8870 wax printer. The lamination process was performed by using a GMP MyJoy-12 laminator (Paju, Korea). A4 size and 100 μM thickness laminate film was purchased from Laminiersysteme (Hollenstedt, Germany). A 40 cm mini-studio shooting tent was sourced from PULUZ Technology Limited (Shenzhen, China). A lamp as a light source for the reflectance measurement was purchased from Micasa Migros (model: 230 V MAX 40 W E27, Zurich, Switzerland). Reflectance measurements were performed by using a Miniature spectrometer (Ocean Optics, Halma plc, Amersham, UK) and OceanView spectrometer software. The light source of the UV−vis spectrometer (SPECORD 250 plus, Analytic Jena, AG, Germany) was used to acquire the spectral sensitivity of the camera loaded onto a smartphone (iPhone XR, Apple, Cupertino, CA).

Fabrication of Paper Substrate. Spots were patterned by a hydrophobic barrier on the paper substrate with a procedure introduced earlier.[5] In this work, the bottom side of the wax-patterned paper substrate was laminated with an A4 sized laminate film. At this time, the upper side of the paper substrate was covered with a baking sheet to prevent the detachment of the laminate.

Preparation of Dye Solution and Dye-Colored Spot on the Paper Substrate. Thioflavin T (ThT) was dissolved in pure water at various concentrations (0, 1.30, 2.60, 3.90, 5.20, 6.50, 10, 25, 50, 100,

DOI: 10.1021/acssensors.9b01802
ACS Sens. 2019, 4, 3093−3101

200, 300, 400, 500, 600, 700, 970, and 1313 mg/L) as stock solutions. Neutral Red (NR) was dissolved in the same way at various concentrations (0.54, 1.09, 1.63, 2.17, 2.72, 5.43, 8.15, 10.87, 13.59, 16.30, 100, 200, 300, 400, 500, and 600 mg/L) and as were Orange IV (1.20, 2.40, 3.60, 4.80, 6.00, 12.00, 120.06, 240.12, 360.18, 480.24, 600.30, and 720.36 mg/L) and Methylene Blue (MB) (100, 200, 300, 400, 500, and 600 mg/L). A volume of 10 μL of stock solution was then added into 2 mL of water in cuvettes for ThT solution analysis with the Canon EOS camera; 4 μL of stock solution was dropped into a 196 μL solution contained in a well of the microtiter plate for ThT, NR, and MB solution analysis with the CanoScan 9000f Mark II scanner, and 8 μL of stock solution was dropped on a paper spot defined by hydrophobic wax barrier for ThT, NR, or Orange IV sample analysis on paper with the same scanner.

Image Data Acquisition by Canon EOS 40D Camera and CanoScan 9000f Mark II Scanner and Data Analysis. A ThT sample solution in cuvette was surrounded by a white paper box whose bottom and front faces were cut out. The camera was set in front of this box and a picture was taken at ISO 400, f/2.8 and sRGB color space. Note that gamma correction is not controllable with this camera. Image data was recorded as CR2 raw data by the camera and subsequently converted into TIFF (16 bit) format by "digital photo professional 4" provided by Canon.

A 96-well plate or ThT-colored paper spots was placed between the cover and the stage of the scanner. In "ScanGear" scanning mode, all the correction settings were turned off while the gamma correction value and color matching were set on demand. Data was taken in TIFF format (48 bit, automatically selected) at 600 dpi.

For image analysis, the color of the image data was split into RGB channels. A circle spot of both ThT solution or paper spot was selected and the mean blue value was acquired by ImageJ software.

Acquisition of Spectral Sensitivity and Absorbance Measurement by Smartphone. As for absorbance measurement. One side of a mini-studio shooting tent was opened and covered with a paper box containing a 1 × 4 cm^2 diagonal opening that served to illuminate the sample. A volume of 10 μL of 100−600 mg/L ThT, NR, or MB solution was mixed with 2 mL of deionized water in a cuvette placed in front of the opening of the shooting tent. Focus and brightness of the smartphone were stabilized manually. The room was otherwise kept completely dark.

To acquire a video of a scanning wavelength lightsource in the range of 370−800 nm, the camera was placed just in front of the light source of the spectrometer while avoiding blockage of the optical pathway for the reference channel. Brightness and focus were fixed manually on the screen of the iPhone XR smartphone during movie acquisition. The UV lamp was turned on, and a 4 nm slit and 10 nm s^{-1} scan rate setting were used.

The conversion of light intensity was done by extracting the sensitivity value at the wavelength closest to the wavelength at which the transmittance was measured (within ±0.1 nm) and multiplying the sensitivity and transmittance values. For best results, the video should be significantly oversampled relative to the spectroscopically acquired spectrum.

Reflectance Measurement. A commercial lamp as a light source, a dye-colored paper substrate, and a probe for reflectance measurement connected to the spectrometer body were placed in a shooting tent box. "OceanView spectroscopy" software was used for data acquisition. With "Active Acquisition" mode, integration time was set to 20 ms with a boxcar width of 11. A tip of the probe where reflected light enters was tilted and stabilized by a clip stand and put on the dye-colored spot of the paper substrate, making the light angle around 100° though the center point of the paper spot. The lamp was set to emit the light source from the diagonal direction to probe through the paper spot. The actual image of the experimental setup is shown in Figure S13.

Prevention of Dye Aggregation on the Paper Substrate. A volume of 2 μL of water was added on each ThT-colored paper spot, and in turn the paper sample was scanned. Scanner conditions and the analysis method were the same as above.

Acquisition of Paper Cross Section. The paper spots colored by 8 μL of 1313 mg/L ThT were cut across the spot diameter and imaged with a Canon EOS 5D Mark III camera equipped with an EF 100 mm f/2.8 L IS USM macro lens with image data in CR2 format.

■ ASSOCIATED CONTENT

Supporting Information

The Supporting Information is available free of charge at https://pubs.acs.org/doi/10.1021/acssensors.9b01802.

Description of XYZ tristimulus values and sRGB (illuminant C) color space conversion; actual analyzed images; image analysis of ThT solution with gamma correction and color matching function; integrated blue-channel corrected light intensity and blue values with and without gamma correction for aqueous phase; example of analysis by red and green channels; RGB absorbance by other color matching functions; original and green- or red-channel corrected light intensity of Methylene Blue and Neutral Red in aqueous phase; results and calculation details of reflectance spectrophotometry; blue values of paper spots; reflectance spectra of Neutral Red on paper substrate; deterioration ratio of ThT on paper substrate; spectra of Orange IV in aqueous phase; cross section of ThT-colored paper spot; experimental setup of the reflectance spectrophotometry (PDF)

■ AUTHOR INFORMATION

Corresponding Author

*E-mail: Eric.Bakker@unige.ch.

ORCID

Eric Bakker: 0000-0001-8970-4343

Author Contributions

All experiments were performed by Y.S. except wax printing on paper substrate done by Chase T. Gerald (ref 5). All authors have given approval to the final version of the manuscript.

Notes

The authors declare no competing financial interest.

■ ACKNOWLEDGMENTS

This work has been supported by the Swiss National Science Foundation.

■ REFERENCES

(1) Martinez, A. W.; Phillips, S. T.; Butte, M. J.; Whitesides, G. M. Patterned Paper as a Platform for Inexpensive, Low-Volume, Portable Bioassays. *Angew. Chem., Int. Ed.* **2007**, *46* (8), 1318−1320.

(2) Morbioli, G. G.; Mazzu-Nascimento, T.; Stockton, A. M.; Carrilho, E. Technical Aspects and Challenges of Colorimetric Detection with Microfluidic Paper-Based Analytical Devices (MPADs) - A Review. *Anal. Chim. Acta* **2017**, *970*, 1−22.

(3) Yamada, K.; Shibata, H.; Suzuki, K.; Citterio, D. Toward Practical Application of Paper-Based Microfluidics for Medical Diagnostics: State-of-the-Art and Challenges. *Lab Chip* **2017**, *17* (7), 1206−1249.

(4) Cate, D. M.; Dungchai, W.; Cunningham, J. C.; Volckens, J.; Henry, C. S. Simple, Distance-Based Measurement for Paper Analytical Devices. *Lab Chip* **2013**, *13* (12), 2397−2404.

(5) Gerold, C. T.; Bakker, E.; Henry, C. S. Selective Distance-Based K^+ Quantification on Paper-Based Microfluidics. *Anal. Chem.* **2018**, *90* (7), 4894−4900.

(6) Cate, D. M.; Noblitt, S. D.; Volckens, J.; Henry, C. S. Multiplexed Paper Analytical Device for Quantification of Metals Using Distance-Based Detection. *Lab Chip* **2015**, *15* (13), 2808−2818.

(7) Soda, Y.; Citterio, D.; Bakker, E. Equipment-Free Detection of K + on Microfluidic Paper-Based Analytical Devices Based on Exhaustive

DOI: 10.1021/acssensors.9b01802
ACS Sens. 2019, 4, 3093−3101

Replacement with Ionic Dye in Ion-Selective Capillary Sensors. *ACS Sens.* **2019**, *4* (3), 670−677.
(8) Li, M.; Tian, J.; Al-Tamimi, M.; Shen, W. Paper-Based Blood Typing Device That Reports Patient's Blood Type "in Writing. *Angew. Chem., Int. Ed.* **2012**, *51* (22), 5497−5501.
(9) Carrasquilla, C.; Little, J. R. L.; Li, Y.; Brennan, J. D. Patterned Paper Sensors Printed with Long-Chain DNA Aptamers. *Chem. - Eur. J.* **2015**, *21* (20), 7369−7373.
(10) Li, J.; Macdonald, J. Multiplex Lateral Flow Detection and Binary Encoding Enables a Molecular Colorimetric 7-Segment Display. *Lab Chip* **2016**, *16* (2), 242−245.
(11) Lewis, G. G.; Robbins, J. S.; Phillips, S. T. A Prototype Point-of-Use Assay for Measuring Heavy Metal Contamination in Water Using Time as a Quantitative Readout. *Chem. Commun.* **2014**, *50* (40), 5352−5354.
(12) Lewis, G. G.; Robbins, J. S.; Phillips, S. T. Point-of-Care Assay Platform for Quantifying Active Enzymes to Femtomolar Levels Using Measurements of Time as the Readout. *Anal. Chem.* **2013**, *85* (21), 10432−10439.
(13) Zhang, Y.; Fan, J.; Nie, J.; Le, S.; Zhu, W.; Gao, D.; Yang, J.; Zhang, S.; Li, J. Timing Readout in Paper Device for Quantitative Point-of-Use Hemin/G-Quadruplex DNAzyme-Based Bioassays. *Biosens. Bioelectron.* **2015**, *73*, 13−18.
(14) Hu, J.; Choi, J. R.; Wang, S.; Gong, Y.; Feng, S.; Pingguan-Murphy, B.; Lu, T. J.; Xu, F. Multiple Test Zones for Improved Detection Performance in Lateral Flow Assays. *Sens. Actuators, B* **2017**, *243*, 484−488.
(15) Karita, S.; Kaneta, T. Acid-Base Titrations Using Microfluidic Paper-Based Analytical Devices. *Anal. Chem.* **2014**, *86* (24), 12108−12114.
(16) Lewis, G. G.; DiTucci, M. J.; Phillips, S. T. Quantifying Analytes in Paper-Based Microfluidic Devices Without Using External Electronic Readers. *Angew. Chem., Int. Ed.* **2012**, *51* (51), 12707−12710.
(17) Jayawardane, B. M.; McKelvie, I. D.; Kolev, S. D. Development of a Gas-Diffusion Microfluidic Paper-Based Analytical Device (MPAD) for the Determination of Ammonia in Wastewater Samples. *Anal. Chem.* **2015**, *87* (9), 4621−4626.
(18) Jansod, S.; Cuartero, M.; Cherubini, T.; Bakker, E. Colorimetric Readout for Potentiometric Sensors with Closed Bipolar Electrodes. *Anal. Chem.* **2018**, *90* (11), 6376−6379.
(19) Soda, Y.; Shibata, H.; Yamada, K.; Suzuki, K.; Citterio, D. Selective Detection of K^+ by Ion-Selective Optode Nanoparticles on Cellulosic Filter Paper Substrates. *ACS Appl. Nano Mater.* **2018**, *1* (4), 1792−1800.
(20) Deng, X.; Smeets, N. M. B.; Sicard, C.; Wang, J.; Brennan, J. D.; Filipe, C. D. M.; Hoare, T. Poly(Oligoethylene Glycol Methacrylate) Dip-Coating: Turning Cellulose Paper into a Protein-Repellent Platform for Biosensors. *J. Am. Chem. Soc.* **2014**, *136* (37), 12852−12855.
(21) Apilux, A.; Siangproh, W.; Praphairaksit, N.; Chailapakul, O. Simple and Rapid Colorimetric Detection of Hg(II) by a Paper-Based Device Using Silver Nanoplates. *Talanta* **2012**, *97*, 388−394.
(22) Chen, G.-H.; Chen, W.-Y.; Yen, Y.-C.; Wang, C.-W.; Chang, H.-T.; Chen, C.-F. Detection of Mercury(II) Ions Using Colorimetric Gold Nanoparticles on Paper-Based Analytical Devices. *Anal. Chem.* **2014**, *86* (14), 6843−6849.
(23) Nilghaz, A.; Guan, L.; Tan, W.; Shen, W. Advances of Paper-Based Microfluidics for Diagnostics - The Original Motivation and Current Status. *ACS Sens.* **2016**, *1* (12), 1382−1393.
(24) Rodman, D. C.; Jarlskog, C. *Spectroscopy and RGB-Colorimetry for Quantification of Plant Pigment and Fruit Content in Fruit Drinks*. B.S. thesis, Lund University, Lund, Sweden, March 2018.
(25) Kuntzleman, T. S.; Jacobson, E. C. Teaching Beer's Law and Absorption Spectrophotometry with a Smart Phone: A Substantially Simplified Protocol. *J. Chem. Educ.* **2016**, *93* (7), 1249−1252.
(26) Özdemir, G. K.; et al. Smartphone-Based Detection of Dyes in Water for Environmental Sustainability. *Anal. Methods* **2017**, *9*, 579−585.
(27) Shen, L.; Ratterman, M.; Klotzkin, D.; Papautsky, I. A CMOS optical detection system for point-of-use luminescent oxygen sensing. *Sens. Actuators, B* **2011**, *155* (1), 430−435.
(28) Priye, A.; Ball, C. S.; Meagher, R. J. Colorimetric-Luminance Readout for Quantitative Analysis of Fluorescence Signals with a Smartphone CMOS Sensor. *Anal. Chem.* **2018**, *90* (21), 12385−12389.
(29) Dhar, A.; Mehta, R.; Sit, M. Colorimetric Detection of pH Strips. *Electrical Engineering and Computer Sciences*; University of California Berkeley, **2017**; EECS 189.
(30) Balas, C. An Imaging Colorimeter for Noncontact Tissue Color Mapping. *IEEE Trans. Biomed. Eng.* **1997**, *44* (6), 468.
(31) Thongprajukaew, K.; Choodum, A.; Sa-E, B.; Hayee, U. Smart Phone: A Popular Device Supports Amylase Activity Assay in Fisheries Research. *Food Chem.* **2014**, *163*, 87−91.
(32) Christodouleas, D. C.; Nemiroski, A.; Kumar, A. A.; Whitesides, G. M. Broadly Available Imaging Devices Enable High-Quality Low-Cost Photometry. *Anal. Chem.* **2015**, *87* (18), 9170−9178.
(33) Dehaene, S. The Neural Basis of the Weber-Fechner Law: A Logarithmic Mental Number Line. *Trends Cognit. Sci.* **2003**, *7* (4), 145−147.
(34) Daina, A.; Michielin, O.; Zoete, V. SwissADME: A Free Web Tool to Evaluate Pharmacokinetics, Drug-Likeness and Medicinal Chemistry Friendliness of Small Molecules. *Sci. Rep.* **2017**, *7*, 42717.
(35) Tucker, S.; Robinson, R.; Keane, C.; Boff, M.; Zenko, M.; Batish, S.; Street, K. W. Colorimetric Determination of pH. *J. Chem. Educ.* **1989**, *66* (9), 769.
(36) Allen, T. C.; Cuculo, J. A. Cellulose Derivatives Containing Carboxylic Acid Groups. *Macromol. Rev.* **1973**, *7* (1), 189−262.
(37) Uejio, J. S.; Schwartz, C. P.; Duffin, A. M.; Drisdell, W. S.; Cohen, R. C.; Saykally, R. J. Characterization of Selective Binding of Alkali Cations with Carboxylate by X-Ray Absorption Spectroscopy of Liquid Microjets. *Proc. Natl. Acad. Sci. U. S. A.* **2008**, *105* (19), 6809−6812.
(38) Zheng, D.; Yuan, X.-A.; Ma, H.; Li, X.; Wang, X.; Liu, Z.; Ma, J. Unexpected Solvent Effects on the UV/Vis Absorption Spectra of *o*-Cresol in Toluene and Benzene: In Contrast with Non-Aromatic Solvents. *R. Soc. Open Sci.* **2018**, *5* (3), 171928.

DOI: 10.1021/acssensors.9b01802
ACS Sens. 2019, 4, 3093−3101